

Short End Effect of Ridge Guide with Planar Circuit Mounted in a Waveguide

YOSHIHIRO KONISHI, SENIOR MEMBER, IEEE, AND HAJIME MATSUMURA

Abstract—The end effect of the short end ridge guide with planar circuit mounted in a waveguide is theoretically obtained by a variational method. The results were also confirmed by measured values. The resonant frequency of a ridge guide resonator was also obtained by using the above mentioned end effect.

I. INTRODUCTION

THE PLANAR CIRCUIT mounted in a waveguide was proposed by Konishi *et al.* [1], [2]. A ridge guide can also be made by this circuit, and this is used for several applications such as a matching circuit and filters. In designing the circuits, it is useful to know the end effect of a short end ridge guide and the resonant frequency of a ridge guide resonator. In this paper, such parameters are theoretically obtained, and the results are confirmed by experimental results.

II. SHORT END RIDGE GUIDE

A short end ridge guide shown in Fig. 1(a) and (b) is sometimes used for a matching circuit in several purposes. In it, the magnetic flux of the ridge guide is disturbed near the short end point, and the magnetic flux invades evanescently in a cutoff waveguide. It results in the taking place of an equivalent inductance jX caused by stored magnetic energy. The equivalent inductance can be modeled by an extended ridge guide, as shown in Fig. 1(c), with the relation

$$X = \tan(\beta\Delta l) \quad (1)$$

where the characteristic impedance of a ridge guide is normalized to 1Ω and Δl is the prolonged length. The value of X or Δl was obtained by a variational method as follows.

When the ridge guide is excited by a dominant mode, the dominant wave is completely reflected from the evanescent region, and the maximum point of voltage lies in the ridge guide. Denoting the discontinuous point by $z=0$ and the maximum point of voltage $z=-l/2$, the electrical field of the dominant ridge guide mode, E_1 takes the value of

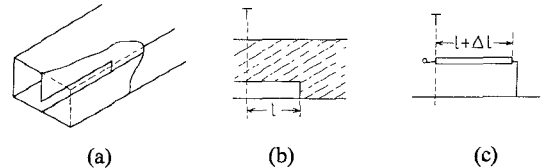


Fig. 1. Construction of a short end ridge guide mounted in a waveguide. (a) A view of the ridge guide with shorted end. (b) The ridge pattern. (c) Equivalent distributed line.

$$E_1 = -jZ_1^{(1)} \cdot \cot\left(\frac{\pi l}{\lambda^{(1)}}\right) e_{1t} \quad (2)$$

where e_{1t} , $Z_1^{(1)}$, and $\lambda^{(1)}$ show the transverse electrical field normalized as (2), the characteristic impedance, and the guide wavelength in the dominant ridge guide mode, respectively. Assuming that the electromagnetic field in the region of $Z < 0$ is just the dominant ridge guide mode, the electric field E_2 and magnetic field H_2 in the region of $Z > 0$ can be calculated from the transverse magnetic field at $Z = -0$, $H_1(-0)$.

That is, E_2 can be obtained as the field radiated from a current distribution J_s at $Z=0$ flowing on the magnetic wall at $Z=0$.

At $Z=+0$, $E_2(+0)$ takes the values of

$$E_2(+0) = - \sum_{n=1}^{\infty} Z_n^{(2)} \langle \mathbf{J}_s \cdot \mathbf{e}_{nt}^{(2)} \rangle \mathbf{e}_{nt}^{(2)} \quad (3)$$

$$\langle |\mathbf{e}_{nt}^{(2)}| \rangle = 1$$

$$\langle \quad \rangle = \int \int_{S'} ds'$$

where $\mathbf{e}_{nt}^{(2)}$, $Z_n^{(2)}$, and S' show the transverse electrical field normalized as (3), the characteristic impedance of the n th mode in the region $Z > 0$, and the cross section of the cutoff waveguide. \mathbf{J}_s , however, should take the values of (4) to keep the continuity of the magnetic field at $Z=0$:

$$\mathbf{J}_s = \mathbf{n} \times \mathbf{h}_{1t} \quad (4)$$

where \mathbf{n} is a normal unit vector toward $Z > 0$ and \mathbf{h}_{1t} is the transverse magnetic field of the dominant ridge guide mode at $Z = -0$. From (3) and (4), we get

Manuscript received November 7, 1977; revised June 15, 1978.

The authors are with the NHK, Technical Research Laboratory, Tokyo, Japan.

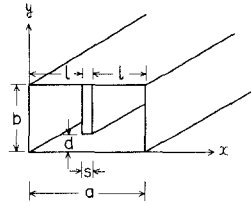
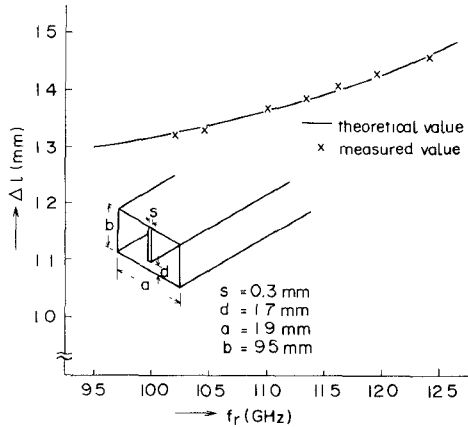


Fig. 2. Dimension of the ridge waveguide.

Fig. 3. Theoretical value and measured value of Δl .

$$E_2(+0) = \sum_{n=1}^{\infty} Z_n^{(2)} \langle \mathbf{e}_{nt}^{(2)} \times \mathbf{h}_{1t} \cdot \mathbf{n} \rangle \mathbf{e}_{nt}^{(2)}. \quad (5)$$

In the above procedure, we have the situation of $\mathbf{E}_1(-0) \neq \mathbf{E}_2(+0)$ although $\mathbf{H}_1(-0) = \mathbf{H}_2(+0)$. This is caused by the neglection of the higher modes in $Z < 0$. We, therefore, can use the variational formula by the concept of reaction [3], or, more generally, variational formula of (6) [4] at $Z = 0$:

$$\iint_{S'} \mathbf{E}_1 \times \mathbf{H}^* \cdot \mathbf{n} \, ds' = \iint_{S'} \mathbf{E}_2 \times \mathbf{H}^* \cdot \mathbf{n} \, ds' \quad (6)$$

$$\mathbf{H} = \mathbf{H}_1(-0) = \mathbf{H}_2(+0).$$

Substituting (2) and (5) into (6), we get

$$jZ_1^{(1)} \cot\left(\frac{\pi l}{\lambda_1^{(1)}}\right) = \sum_{n=1}^{\infty} Z_n^{(2)} \langle \mathbf{e}_{nt}^{(2)} \times \mathbf{h}_{1t} \cdot \mathbf{n} \rangle^2 = -jX \quad (7)$$

$$Z_n^{(2)} = \frac{j\omega\mu}{\gamma_n^{(2)}} \quad (\text{TE mode})$$

$$= \frac{\gamma_n^{(2)}}{j\omega\epsilon} \quad (\text{TM mode}). \quad (8)$$

Since the left-hand side of (7) is the impedance toward $Z > 0$ at $Z = 0$, the right-hand side shows the values of X .

In (8), the values of $\gamma_n^{(2)}$ take the positive real numbers as the region $Z > 0$ corresponds to a cutoff waveguide. Therefore, the values of X can be calculated by (7) as a function of ω .

In a practical case, X is much smaller than $Z_1^{(1)}$, and the condition of $\cot(\pi l/\lambda_1^{(1)}) \ll 1$ can be used. Therefore, the

left hand side of (7) can be expanded by using the relation of $\Delta l = (\lambda_1^{(1)}/4) - (l/2)$. It gives us the relation of

$$\Delta l = \frac{\lambda_1^{(1)} \sum_{n=1}^{\infty} Z_n^{(2)} \langle \mathbf{e}_{nt}^{(2)} \times \mathbf{h}_{1t} \cdot \mathbf{n} \rangle^2}{j2\pi Z_1^{(1)}}. \quad (9)$$

It can apply to any ridge guide line of a short end side in Fig. 1. For an example, we used the expression of (10) for a dominant ridge guide mode in the structure of Fig. 2 [5] and the mode expression of (11) for TE and TM modes in the region $Z > 0$:

$$h_{1y} = A \sum_{n=1}^{\infty} P_n \cosh(\gamma_n x) \sin\left(\frac{n\pi y}{b}\right)$$

$$h_{1x} = A \left\{ Q \sin(k_c x) + \sum_{n=1}^{\infty} R_n \sin(\gamma_n x) \cos\left(\frac{n\pi y}{b}\right) \right\}$$

$$\gamma_n^2 = \left(\frac{n\pi}{b}\right)^2 - \left(\frac{2\pi}{\lambda_c}\right)^2$$

$$P_n = \frac{2 \sin\left(\frac{n\pi d}{b}\right)}{b\gamma_n \sinh(\gamma_n l)} \cos\left(\frac{k_c s}{2}\right)$$

$$Q = \frac{d}{b \sin(k_c l)} \cos\left(\frac{k_c s}{2}\right)$$

$$R_n = \frac{2 \sin\left(\frac{n\pi d}{b}\right)}{n\pi \sinh(\gamma_n l)}$$

$$2A^2 \int_0^l \int_0^b (h_{1y}^2 + h_{1x}^2) \, dx \, dy = 1$$

$$k_c = \frac{2\pi}{\lambda_c} \quad (10)$$

$$e_{mny}^{(2)} = -A_{mn} \frac{m\pi}{l} \sin\left(\frac{m\pi x}{l}\right) \cos\left(\frac{n\pi y}{b}\right)$$

$$e_{mnx}^{(2)} = A_{mn} \frac{n\pi}{b} \cos\left(\frac{m\pi x}{l}\right) \sin\left(\frac{n\pi y}{b}\right)$$

$$A_{mn} = \frac{2}{\sqrt{2lb} \sqrt{\left(\frac{m\pi}{l}\right)^2 \epsilon_n + \left(\frac{n\pi}{b}\right)^2}} \quad \epsilon_0 = 2 \quad \epsilon_n (n \geq 1) = 1. \quad (11)$$

The computed result is shown as a line in Fig. 3. The experimental result points in Fig. 3 that are obtained from the measurement of the resonant frequency in a ridge guide, as mentioned in the next section, show good agreement with the theoretical line.

III. RESONANT FREQUENCY OF A RIDGE GUIDE RESONATOR

A sketch of a ridge guide resonator formed by a planar circuit mounted in waveguide is shown in Fig. 4. For a half-wavelength resonator, the center of a ridge guide becomes a magnetic wall, and (7) can also be used for

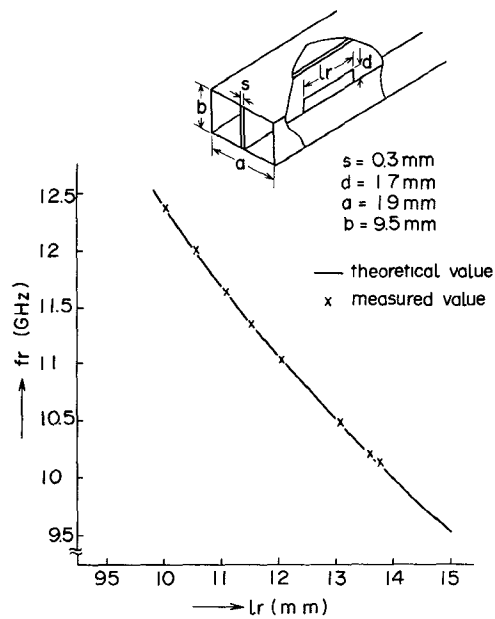


Fig. 4. Theoretical value and measured value of resonant frequency of the ridge guide resonator with planar circuit of mounted waveguide.

obtaining the resonant frequency by considering the end effect and the guided wave length of a ridge guide as (12):

$$\frac{\lambda_1^{(1)}(\omega)}{2} = l_r + 2\Delta l. \quad (12)$$

Since $\lambda_1^{(1)}$ and Δl of (12) are the functions of ω , the values of the resonant frequency were calculated by computer. The results and the measured values are shown in Fig. 4.

REFERENCES

- [1] Y. Konishi *et al.*, "New microwave components with mounted planar circuit in waveguide," IECE Japan, MW72-84, Oct. 1972.
- [2] —, "The design of a bandpass filter with inductive strip—Planar circuit mounted in waveguide," *IEEE Trans. Microwave Theory Tech.*, vol. MTT-22, pp. 869–873, Oct. 1974.
- [3] R. F. Harrington, *Time-Harmonic Electromagnetic Fields*. New York: McGraw-Hill, 1961.
- [4] Y. Konishi, *Electromagnetic Wave Circuit* (in Japanese). Ohm Co., 1976.
- [5] W. J. Getsinger, "Ridge waveguide field description and application to directional couplers," *IRE Trans. Microwave Theory Tech.*, vol. MTT-10, pp. 41–51, Jan. 1962.

Propagation Through Hollow Cylindrical Anisotropic Dielectric Guides

B. B. CHAUDHURI AND D. K. PAUL

Abstract—Hybrid mode in a circular hollow anisotropic dielectric guide is reported here. The use of such guide in fabricating gas laser is compared with its isotropic counterpart. It has been shown that proper choice of anisotropic material can increase the net gain of gas lasers.

HOLLOW dielectric waveguides at optical and infrared frequency have found wide use in high-pressure laser oscillators and amplifiers. The waveguides are low-loss if the cross-section dimensions are many wavelengths and the interior walls have an optical finish. However, the gain of the amplifier falls approximately as the square root of the cross-sectional area, so that there is an optimum dimension for which net gain is maximum. Isotropic hollow guides have been analyzed by different authors [1], [2].

The following note analyzes hollow circular waveguide with anisotropic dielectric, where it has been shown that

for the dominant hybrid mode HE_{11} at 6328 \AA a net gain of 1.5 dB/m over that of the isotropic guide can be achieved by proper choice of anisotropy.

Consider a hollow waveguide of radius r_0 with axis coinciding with the z -axis of (r, ϕ, z) coordinate system. The surrounding medium has dielectric constants ϵ_z in z -direction and ϵ_r in the transverse plane. Solving Maxwell's equation and applying boundary condition to the fields, we arrive at the following transcendental equation:

$$\begin{aligned} & \left[\frac{1}{u} \frac{J'_n(u)}{J_n(u)} - \frac{1}{v_1} \frac{H'_n(v_1)}{H_n(v_1)} \right] \left[\frac{1}{u} \frac{J'_n(u)}{J_n(u)} - \frac{\bar{\epsilon}_z}{v_2} \frac{H'_n(v_2)}{H_n(v_2)} \right] \\ &= \left(\frac{nh}{K_0} \right)^2 \cdot \frac{\left(\frac{u^2}{a^2} - v_2^2 \right) (u^2 - v_1^2)}{u^4 v_1^2 v_2^2} \quad (1) \end{aligned}$$

where h is the propagation constant in the z -direction and

Manuscript received November 22, 1977; revised May 4, 1978.

The authors are with the Department of Electrical Engineering, Indian Institute of Technology Kanpur, Kanpur-208 016, U.P., India.